



ARTICLE

In-Plane Impact Dynamics Analysis of Re-Entrant Honeycomb with Variable Cross-Section

Yuanxun Ou^{1,2}, Shilin Yan^{1,2} and Pin Wen^{1,2,*}

¹Department of Engineering Structure and Mechanics, Wuhan University of Technology, Wuhan, 430070, China

²Hubei Key Laboratory of Theory and Application of Advanced Materials Mechanics, Wuhan, 430070, China

*Corresponding Author: Pin Wen. Email: wenpin@whut.edu.cn

Received: 02 November 2020 Accepted: 11 December 2020

ABSTRACT

Due to the unique deformation characteristics of auxetic materials (Poisson's ratio $\mu < 0$), they have better shock resistance and energy absorption properties than traditional materials. Inspired by the concept of variable cross-section design, a new auxetic re-entrant honeycomb structure is designed in this study. The detailed design method of re-entrant honeycomb with variable cross-section (VCRH) is provided, and five VCRH structures with the same relative density and different cross-section change rates are proposed. The in-plane impact resistance and energy absorption abilities of VCRH under constant velocity are investigated by ABAQUS/EXPLICIT. The results show that the introduction of variable cross-section design can effectively improve the impact resistance and energy absorption abilities of auxetic re-entrant honeycombs. The VCRH structure has better Young's modulus, plateau stress, and specific energy absorption (SEA) than traditional re-entrant honeycomb (RH). The influence of microstructure parameters (such as cross-section change rate α) on the dynamic impact performance of VCRH is also studied. Results show that, with the increase in impact velocity and α , the plateau stress and SEA of VCRH increase. A positive correlation is also found between the energy absorption efficiency, impact load uniformity and α under both medium and high impact speeds. These results can provide a reference for designing improved auxetic re-entrant honeycomb structures.

KEYWORDS

Auxetic re-entrant honeycombs; variable cross-section design; in-plane impact; finite element simulation

1 Introduction

Different from traditional materials, auxetic materials (Poisson's ratio $\mu < 0$) are wider perpendicular to the tensile direction, and narrower perpendicular to the compression direction. Due to their great advantages in shear resistance, indentation resistance, fracture resistance and energy absorption properties [1–4], auxetic materials have been applied in various fields, including sound insulation, shock absorber, sandwich panel composite core and artificial prosthesis [5–8]. Various microstructure models have been developed to enhance the mechanical properties of auxetic materials [4]. Especially in the impact process, the dynamic response characteristics of auxetic re-entrant honeycomb are heavily dependent on its non-uniform deformation. Moreover,



the cellular structure has a great influence on the evolution of macro/micro dynamic stress [1]. Therefore, researchers are continually focused on designing better cell structure to enhance the impact resistance and impact energy absorption abilities of auxetic material, and to ultimately achieve better dynamic performance in line with the engineering requirements.

Significant efforts have been made by researchers to study the relationship between the geometric structure and mechanical properties of auxetic material. Xiao et al. [9] predicted the crashworthiness of re-entrant auxetic honeycomb under quasi-static loads and dynamic loads of different impact velocities by using finite element method. The results showed that different load conditions have great influence on the load-bearing, energy absorption and deformation modes of re-entrant auxetic honeycomb. Hu et al. [10] and Hou et al. [11] analyzed the cell structure parameters of re-entrant auxetic honeycomb, including cell wall angle, ratio of wall thickness to wall length, etc. Tan et al. [12] designed two levels of re-entrant auxetic honeycomb based on hexagon substructure and equilateral triangle substructure. It was found that the designed re-entrant auxetic honeycomb has higher energy absorption capacity. Dong et al. [13] studied the influence of wall thickness on re-entrant auxetic honeycomb deformation mode and the effect of negative Poisson's ratio on crushing stress through experimental and numerical methods. They found that there are great differences in deformation modes and energy absorption between re-entrant auxetic honeycomb with thin-wall and thick-wall. Sun et al. [14] proposed a multi-functional layered honeycomb structure, whose mechanical properties such as Young's modulus were derived based on the Euler beam theory. Lu et al. [15] designed a new honeycomb structure with a narrow rib in the inner concave honeycomb structure. Fu et al. [16] derived the analytical solutions of equivalent Young's modulus and Poisson's ratio for a new chiral three-dimensional auxetic material by using beam theory. Li et al. [17] designed a two-dimensional multi-level concave honeycomb structure, and studied its energy absorption effect under different levels by finite element method. Hou et al. [18] improved the two-dimensional multi-level concave honeycomb structure. Then, they used the finite element method to analyze the dynamics of the improved honeycomb structure in order to further improve the energy absorption effect. Zhang et al. [19] proposed a bio-inspired re-entrant arc-shaped honeycomb, and studied the influence of cellular microstructure on its impact dynamic response characteristics. The above literature review shows the mechanical behavior of auxetic re-entrant honeycombs has been widely studied, but most of the previous studies assume that the cross-section of the structure remains unchanged. There are few studies on auxetic re-entrant honeycomb with variable cross-section.

Recently, some researchers have introduced the idea of variable cross-section, which can improve the impact resistance and energy absorption abilities of structures. In order to improve the crashworthiness of the front longitudinal beam (S-shaped thin-walled beam), Xu et al. [20] designed a variable cross-section S-shaped thin-walled beam. Zhang et al. [21] proposed a kind of multi-cell thin-walled structure with variable cross-section, and studied the influence of wall thickness on its energy absorption abilities. Xiaofei et al. [22] proposed a new rhombic dodecahedron lattice structure with variable cross section, which has better mechanical properties and energy absorption than the original one.

In this paper, based on the variable cross-section design concept and the traditional re-entrant honeycomb structure, a re-entrant honeycomb with variable cross-section (VCRH) was proposed. Different cell wall structures were designed to improve the impact resistance and energy absorption abilities. Then, the dynamic mechanical behavior of VCRH was compared to that of traditional re-entrant honeycomb (RH). Finally, the effects of impact velocity and cell microstructure on the impact deformation characteristics, plateau stress and specific energy absorption (SEA) of VCRH

were studied by numerical simulation. This study provides a new way to improve the mechanical properties and impact resistance of cellular materials.

2 Design of Structures

The cell structures of RH and VCRH are shown in Fig. 1. The geometric dimensions of inclined cell wall length l , horizontal cell wall length a and inclined cell wall angle θ of the two cell structures are consistent. In this study, $l = 20$ mm, $a = 10$ mm, and $\theta = 120^\circ$. All cell walls of RH cells have uniform cross-section with thickness of t , while horizontal cell walls of VCRH cells have variable cross-section. The maximum and minimum thicknesses are found at both ends and at the middle of the horizontal cell wall, which are t_1 and t_2 respectively.

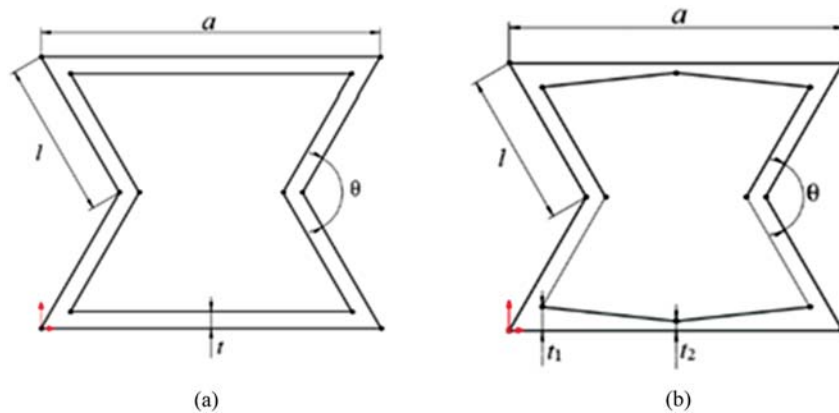


Figure 1: Unit cell structures: (a) RH, (b) VCRH

Different from other materials, the most important characteristic of a cellular material is its relative density. The purpose of using the relative density is to eliminate the influence of the mass of porous structure on the mechanical properties. The relative density is defined as follows:

$$\Delta\rho = \frac{\rho_0}{\rho_s} \tag{1}$$

where ρ_0 is the initial density and ρ_s is the material density of the structures. For the RH structure, the formula for calculating the relative density is as follows:

$$\Delta\rho = \frac{(2l + a)t}{la \sin\frac{\theta}{2}} \tag{2}$$

The VCRH cell is composed of two kinds of cell walls, including four inclined cell walls with uniform cross-section and two horizontal cell walls with variable cross-section. The relative density of honeycomb with variable cross-section can be given by the following formula:

$$\Delta\rho = \frac{4S_1 + 2S_2}{ab} \tag{3}$$

where S_1 and S_2 represent the areas of inclined and horizontal cell walls:

$$S_1 = lt \tag{4}$$

$$S_2 = \frac{(t_1 + t_2)(a - \frac{t}{\sin\theta} + \frac{t}{\tan\theta})}{2} - \frac{t_1^2}{\tan\theta} \quad (5)$$

In order to quantify the change in horizontal cell wall cross-section, the cross-section change rate α is proposed:

$$\alpha = 1 - \frac{t_2}{t_1} = \frac{t_1 - t_2}{t_1} \quad (6)$$

The cross-section change rate α ranges from 0 to 1. The VCRH will degenerate into RH when $\alpha = 0$. In the following research, the effective relative density $\Delta\rho$ remains unchanged. Notably, the relative density is not exactly the same due to errors. Different combinations of thickness t_1 and t_2 are selected to obtain the representative α . Tab. 1 lists all the cellular configurations considered.

Table 1: Geometric parameters of VCRH

Sample	$\Delta\rho$	t_1	t_2	α
VCRH-1	0.2235	1	1	0
VCRH-2	0.2236	1.11	0.89	0.2
VCRH-3	0.2238	1.25	0.75	0.4
VCRH-4	0.2237	1.42	0.57	0.6
VCRH-5	0.2241	1.65	0.33	0.8

3 Finite Element Simulation Analysis

3.1 Finite Element Model

In order to analyze the influence of cross-section change rate α on the impact resistance and energy absorption abilities of VCRH, ABAQUS/EXPLICIT software was used to simulate the conventional and new-type re-entrant honeycomb structures. The finite element model of VCRH is shown in Fig. 2 (taking VCRH-1 for example). The matrix material in the numerical simulation is aluminum with density ρ of 2700 kg/m³, Young's modulus E of 69 GPa, and Poisson's ratio ν of 0.3. The ideal elastic-plastic model obeys Mises yield criterion, where yield stress σ_{ys} is set to 76 MPa. In the simulation process, the supporting rigid plate is fixed by setting the reference point degree of freedom to 0, and the upper rigid plate is squeezed vertically by constant impact load. The mass of impacting rigid plate is 20 kg. The honeycomb is modeled by three node plane stress triangular element (cps3). The out of plane thickness of honeycomb structure is 10 mm, so the plane stress/strain thickness is set to 10. General contact is applied on the surfaces of the model. In addition, face-to-face contact is made between the VCRH structure and the two rigid plates, and the friction coefficient is set to 0. The free boundary is adopted for left and right edges of the sample.

3.2 Key Performance Indicators

The nominal stress-strain curve (solid line) of the VCRH is shown in Fig. 3. As seen from the figure, the process of deformation can be divided into three stages: the initial elastic deformation of honeycomb, progressive plastic yield of honeycomb cell, and significant amount of cell yield which leads to densification. Plateau stress (σ_m) is an important index to evaluate the energy absorption abilities of cellular structures. The plateau stress value of cellular structure can be

obtained by taking the average value of the platform stage stress in the stress–strain curve, which can be expressed as follows:

$$\sigma_m = \frac{1}{\epsilon_d - \epsilon_y} \int_{\epsilon_y}^{\epsilon_d} \sigma(\epsilon) d\epsilon \quad (7)$$

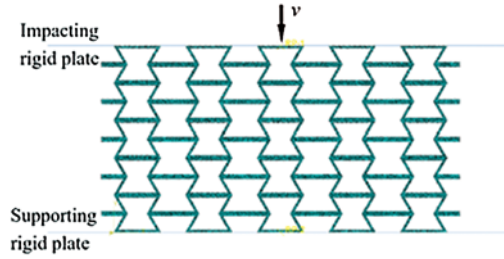


Figure 2: Finite element model of VCRH-1

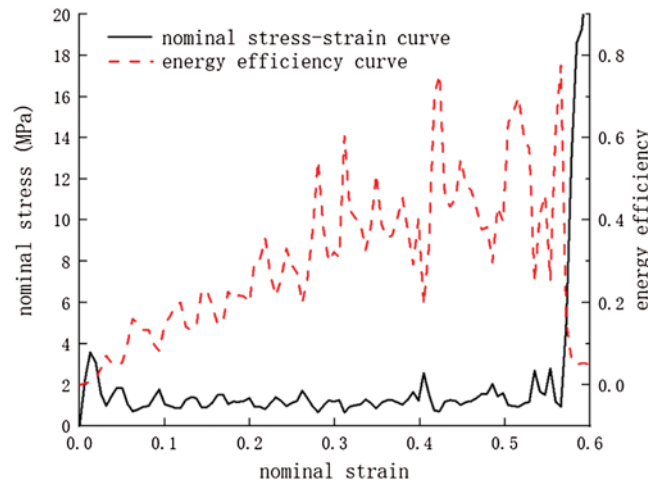


Figure 3: Nominal stress–strain curve and energy absorption efficiency curve of VCRH

Here, $\sigma(\epsilon)$ represents the change in nominal stress with the strain; ϵ_y represents the nominal strain corresponding to the peak value of initial stress, which is set to be 0.02 here; and ϵ_d is the maximum strain before the material is compressed and compacted. Previous research shows that the densification strain ϵ_d is largely decided by the impact velocity and the topological structure of the cell [23]. In order to eliminate the influence of subjective factors, the densification strain was obtained by energy absorption efficiency method:

$$\frac{d}{d\epsilon} \left[\frac{1}{\sigma(\epsilon)} \int_0^\epsilon \sigma(\epsilon) d\epsilon \right] \Big|_{\epsilon=\epsilon_d} = 0 \quad (8)$$

As shown in Fig. 3, there are many local peaks in the energy efficiency curve. The nominal strain corresponding to the final peak value (i.e., the point at which the energy efficiency curve begins to decline rapidly) is regarded as the densification strain. In order to study the impact

resistance and energy absorption abilities of VCRH, the following key performance indicators based on densification strain are proposed.

A cellular material with good impact behavior should maintain impact load uniformity during impact. In other words, the maximum stress peak value should be less than the damage critical value, and the fluctuation of stress should be as small as possible. The impact load efficiency (ILE) represents the impact load uniformity of cellular material, which is expressed as:

$$ILE = \frac{\sigma_m}{\sigma_{max}} \quad (9)$$

Here, σ_{Max} and σ_m are two parameters corresponding to the nominal stress–strain curve, the maximum peak stress and the plateau stress. In order to obtain better energy absorption structure, the value of σ_{Max} should be smaller and the value of ILE should be higher. For an ideal energy absorbing structure, $ILE = 1$, which means σ_{Max} is equal to σ_m . The minimum cushioning coefficient C_{min} is an evaluation index of honeycomb structure crashworthiness, which is defined as:

$$C_{min} = \frac{1}{ILE \times \varepsilon_d} \quad (10)$$

Here, C_{min} represents the energy absorption efficiency of honeycomb structure under the impact load. The impact resistance of honeycomb structure is negatively correlated with the value of C_{min} .

In order to evaluate the energy absorption abilities of honeycomb structure, specific energy absorption (SEA) is defined as the ratio of total energy absorption to mass:

$$SEA = \frac{V \int_0^{\varepsilon_d} \sigma(\varepsilon) d\varepsilon}{m} = \frac{\int_0^{\varepsilon_d} \sigma(\varepsilon) d\varepsilon}{\rho_0} \quad (11)$$

where m , V and ρ_0 are the mass, volume and density of the honeycomb model, respectively.

3.3 Analysis of Mesh Sensitivity

In this part, the accuracy and reliability of numerical simulation are verified. In order to verify the accuracy and reliability of the finite element model, the deformation mode of traditional re-entrant honeycomb under impact load is simulated and compared with the literature results [24]. Fig. 4 shows the deformation comparison between the simulation results and the literature results under dynamic impact load ($v = 20$ m/s). When the impact velocity, material properties and geometric parameters are the same, the local deformation and global deformation of the simulation results are in good agreement with the literature results [24].

Before the simulation, the sensitivity of the numerical results to the mesh size was analyzed. Fig. 5 shows the effect of element size on the plateau stress and the calculation time. The results show that when the element size decreases to 1 mm, the platform stress tends to be stable and converges gradually. However, with the decrease in element size, the calculation time increases rapidly. Considering the accuracy and efficiency of finite element simulation, the mesh size of honeycomb structure is set as 0.5 mm. A large number of convergence tests show that the existing finite element model is accurate and effective, and is suitable to analyze the dynamic characteristics and energy absorption performance of honeycomb structures under impact load. Therefore, the finite element model described above is reliable and can be used for subsequent research.

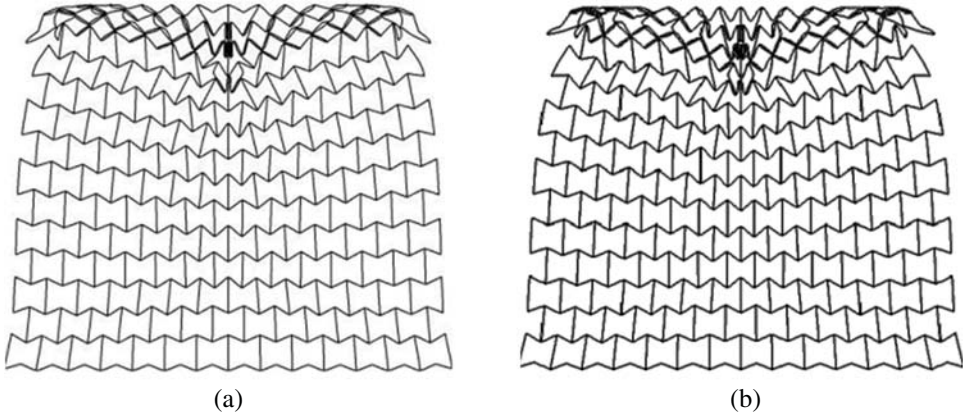


Figure 4: Comparison of impact deformation for traditional re-entrant honeycomb at $v = 20$ m/s (a) the simulation results and (b) the reference results

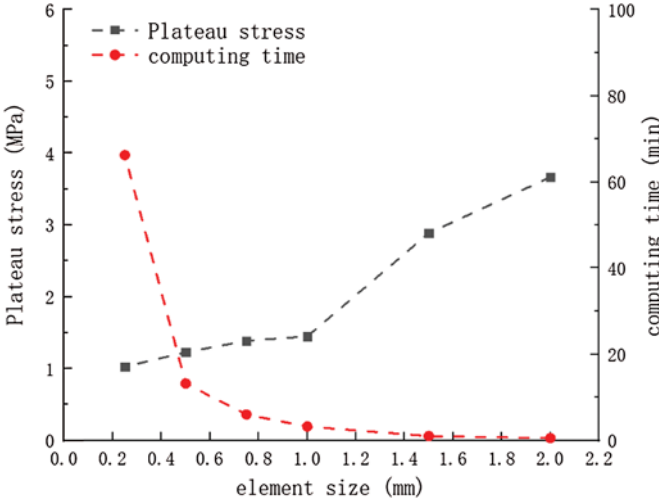


Figure 5: Effect of element size on plateau stress and calculation time of VCRH

4 Results and Discussion

4.1 Deformation Mode

In order to study the influence of the cross-section change rate α on the deformation mode of the re-entrant honeycomb structure, the in-plane impact numerical simulation with velocity of 20 m/s was carried out for all the designed samples. Fig. 6 shows the deformation mode and stress distribution of conventional and VCRH structures under in-plane impact. At the initial stage of impact, when $\epsilon = 0.1$, the deformation of honeycomb structure is concentrated on the cell unit near the impact end, and the “necking” phenomenon occurs at the two free surfaces of the impact end. When the strain increases gradually, the shock wave cannot propagate to the bottom of the model in a short time due to the high velocity, so it is mainly concentrated near the impact end. In other words, the cells closest to the impact end deform greatly, while the other cell units of the model are not deformed to a great extent. Therefore, the cell units of the model are crushed layer by layer.

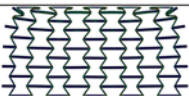
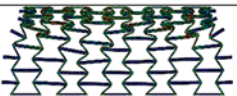
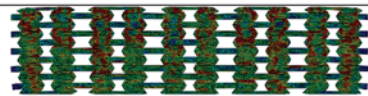
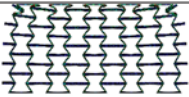
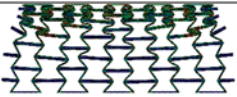
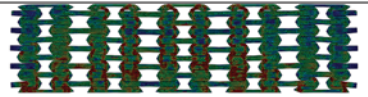
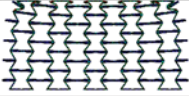
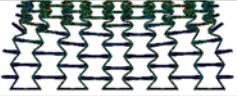
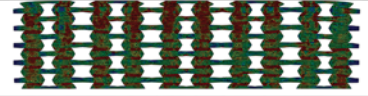
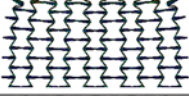
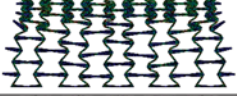
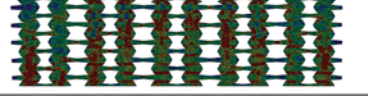
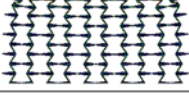
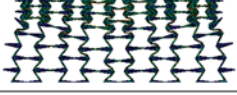
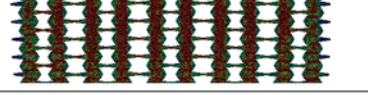
Sample	$\varepsilon = 0.1$	$\varepsilon = 0.3$...	At crushing strain
VCRH-1			...	
VCRH-2			...	
VCRH-3			...	
VCRH-4			...	
VCRH-5			...	

Figure 6: Deformation mode comparison of VCRH structures through simulation results

It can be seen from Fig. 6 that the VCRH can enter the deformation mode of layer-by-layer collapse more quickly, which means the cells nearest to the impact end are crushed more quickly. This is mainly because the two ends of horizontal cell wall of VCRH cell are thicker, and the strain value required for cell collapse is smaller. Fig. 7 shows the comparison of the deformation modes of VCRH unit cells at crushing strain. Tab. 2 shows the strain of re-entrant cellular structure under different cross-section change rates. The larger the cross-section change rate α , the earlier the complete collapse stage appears.

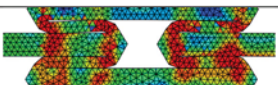
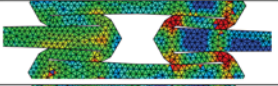
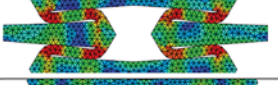
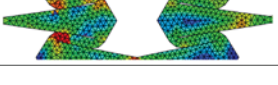
Sample	At crushing strain
VCRH-1	
VCRH-2	
VCRH-3	
VCRH-4	
VCRH-5	

Figure 7: Deformation mode comparison of VCRH unit cells at crushing strain

Table 2: Crushing strain data of VCRH structures

Sample	VCRH-1	VCRH-2	VCRH-3	VCRH-4	VCRH-5
Crushing strain	0.591	0.578	0.566	0.546	0.509

4.2 Mechanical Characteristics of VCRH

4.2.1 Young's Modulus

In order to obtain the elastic modulus of the structure, the quasi-static compression simulation of the model was carried out. The total displacement of top surface of VRCH is assumed to be 1 mm under the loading rate of 0.6 mm/min. In this case, the elastic moduli of five models with different values of cross-section change rate α are given in Tab. 3. As can be seen, there is a positive correlation between the elastic modulus and α .

Table 3: Young's modulus values of VCRH structures

Sample	VCRH-1	VCRH-2	VCRH-3	VCRH-4	VCRH-5
Young's modulus (MPa)	396	437	489	556	761

4.2.2 Plateau Stress

According to Eq. (7), the effects of cross-section change rate α and impact velocity on the plateau stress σ_m of VCRH are studied. Fig. 8 shows the change in plateau stress relative to α under different impact loads. The results show that the plateau stress of VCRH structure is greater than that of RH structure. When the impact velocity is constant, the plateau stress increases with α . For the honeycomb structure with the same α , the plateau stress increases with impact velocity.

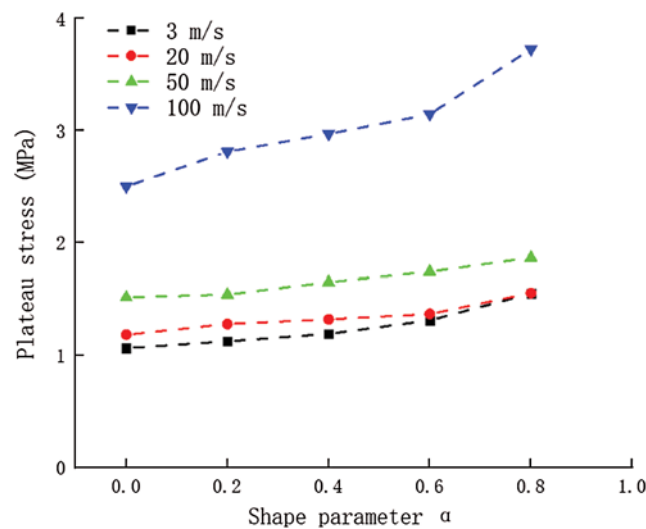


Figure 8: Effect of cross-section change rate α on plateau stress of VCRH under different impact velocities

4.2.3 Impact Load Uniformity

As a critical indicator for good impact resistant structure, the impact load uniformity of VCRH was also investigated. The dynamic response curves of VCRH structure with cross-section change rate $\alpha = 0.8$ and RH structure at $v = 20$ m/s are shown in Fig. 9. Due to the introduction of variable cross-section cell wall structure, the maximum peak stress of VCRH structure is less than that of RH structure under the same impact velocity.

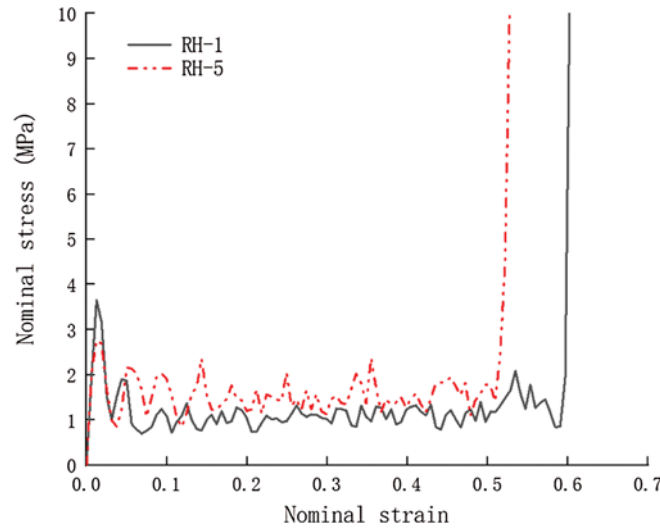


Figure 9: Dynamic response curves of VCRH-1 and VARH-5

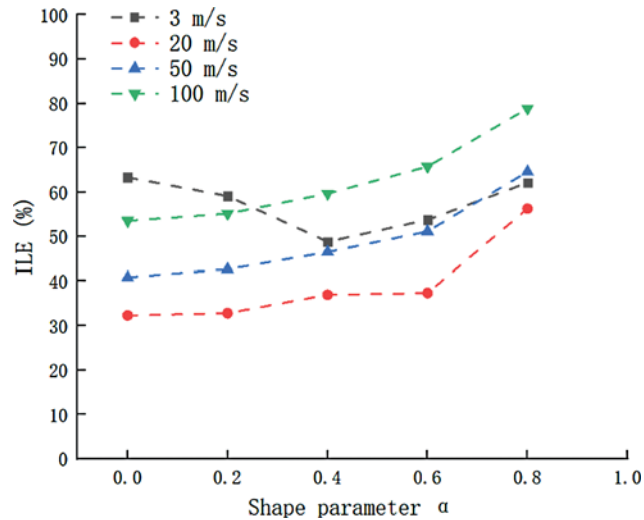


Figure 10: Effect of cross-section change rate α on ILE of VCRH under different impact velocities

The impact load uniformity is quantified as ILE for better understanding the influence of cross-section change rate α on the energy absorbing ability of VRCH. Fig. 10 shows the curve of α vs ILE under different impact velocities. At low velocity impact ($v = 3$ m/s), ILE decreases first and then increases with α . Especially when $\alpha = 0.8$, the crush load uniformity of VCRH structure is the same as that of RH structure. However, under the conditions of medium velocity ($v = 20$ m/s, $v = 50$ m/s) and high-speed impact ($v = 100$ m/s), the impact load uniformity of VCRH structure is better than that of RH structure, and the ILE of VCRH structure increases with α .

4.3 Energy Absorption Characteristics

In order to evaluate the energy absorption efficiency of honeycomb structure, the minimum dynamic cushioning coefficient (C_{min}) is proposed. C_{min} is inversely proportional to the cushioning performance of honeycomb. Fig. 11 shows the effect of cross-section change rate α on C_{min} of VCRH structure at different impact velocities. At low velocity impact ($v = 3$ m/s), C_{min} , like the ILE, increases first and then decreases with α . Under the conditions of medium velocity ($v = 20$ m/s, $v = 50$ m/s) and high-speed impact ($v = 100$ m/s), the C_{min} of the new honeycomb structure decreases with the increase in value of α . Under the condition of medium and high velocity impact, C_{min} decreases with the increase in impact velocity for re-entrant honeycomb structure with the same α .

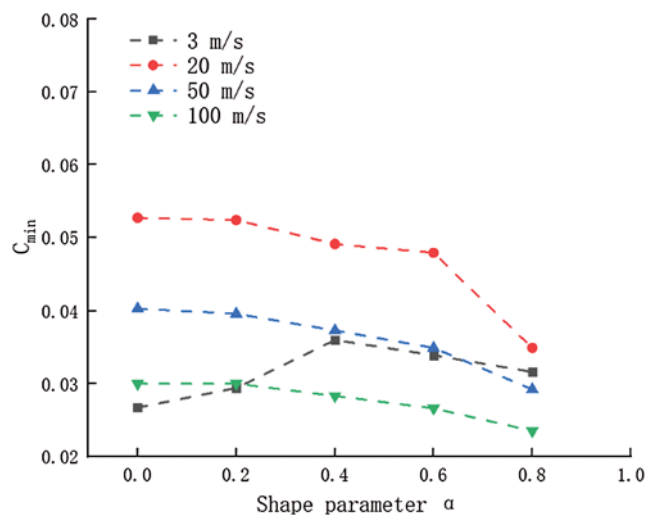


Figure 11: Effect of cross-section change rate α on C_{min} of VCRH under different impact velocities

Fig. 12 shows the effect of cross-section change rate α on the specific energy absorption (SEA) of VCRH under different impact velocities. The results show that the SEA of VCRH structure is greater than that of RH structure, that is, the VCRH structure has better energy absorption characteristics. The SEA increases with α under the same impact velocity. For the honeycomb structure with the same α , the SEA increases with impact velocity.

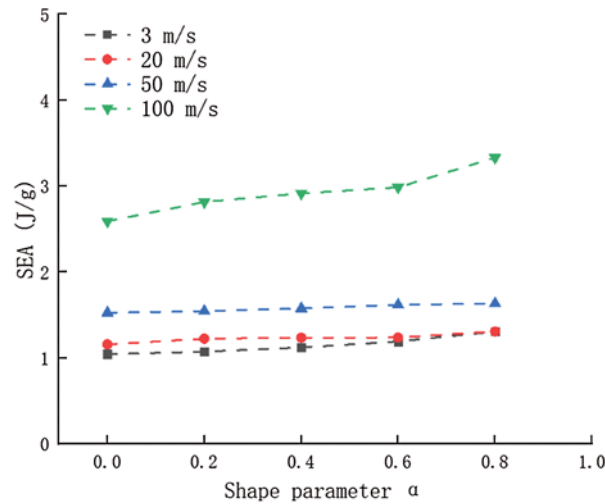


Figure 12: Effect of cross-section change rate α on SEA of VCRH under different impact velocities

5 Conclusions

In this study, a re-entrant honeycomb with variable cross-section (VCRH) is proposed based on the concept of variable cross-section design. Compared with the traditional re-entrant honeycomb (RH), the impact resistance and energy absorption of VCRH are significantly improved. The dynamic impact response and energy absorption characteristics of VCRH under different in-plane impact velocities are evaluated by studying the micro-structure parameters. The main conclusions of this paper are obtained by simulation analysis.

The deformation mode of honeycomb structure is determined by impact velocity and cell microstructure. The introduction of variable cross-section into RH leads to the change in macro/micro deformation characteristics during impact. Compared with RH, VCRH can enter the complete collapse stage earlier. Moreover, the crushing strain of VCRH is negatively correlated with the cross-section change rate α .

Compared with RH, the elastic modulus of the VCRH structure is significantly increased. In addition, at the same impact velocity, the VCRH has higher dynamic platform pressure and SEA than the RH. It is found that the RH has better impact load uniformity and energy absorption efficiency at low speed, while the VCRH structure has better impact load uniformity and energy absorption efficiency at medium and high speed. The results also show that the dynamic platform pressure and SEA are positively correlated with the cross-section change rate. At medium and high impact velocities, the impact load uniformity and energy absorption efficiency are positively correlated with the cross-section change rate. These results can provide a reference for designing improved auxetic re-entrant honeycomb structures.

Funding Statement: This research is supported by the National Natural Science Foundation of China (No. 11902232).

Conflicts of Interest: The authors declare that they have no conflicts of interest to report regarding the present study.

References

1. Gibson, L. J., Ashby, M. F. (1997). *Cellular solids: Structure and properties*. Cambridge: Cambridge University Press.
2. Sun, Y., Li, Q. M. (2018). Dynamic compressive behaviour of cellular materials: A review of phenomenon, mechanism and modelling. *International Journal of Impact Engineering*, 112(2), 74–115. DOI 10.1016/j.ijimpeng.2017.10.006.
3. Ren, X., Shen, J., Tranc, P., Ngo, T. D., Xie, Y. M. (2018). Design and characterisation of a tuneable 3D buckling-induced auxetic metamaterial. *Materials & Design*, 139(2), 336–342. DOI 10.1016/j.matdes.2017.11.025.
4. Lim, T. C. (2015). *Auxetic materials and structures*. Singapore: Springer.
5. Bertoldi, K., Reis, P. M., Willshaw, S., Mullin, T. (2010). Negative Poisson's ratio behavior induced by an elastic instability. *Advanced Materials*, 22(3), 361–366. DOI 10.1002/adma.200901956.
6. Ma, Y., Scarpa, F., Zhang, D., Zhu, B., Chen, L. et al. (2013). A nonlinear auxetic structural vibration damper with metal rubber particles. *Smart Materials & Structures*, 22(8), 084012. DOI 10.1088/0964-1726/22/8/084012.
7. Wu, Y., Liu, Q., Fu, J., Li, Q., Hui, D. (2017). Dynamic crash responses of bio-inspired aluminum honeycomb sandwich structures with CFRP panels. *Composites Part B Engineering*, 121b(7), 122–133. DOI 10.1016/j.compositesb.2017.03.030.
8. Scarpa, F. (2008). Auxetic materials for bioprotheses. *IEEE Signal Processing Magazine*, 25(5), 128–126. DOI 10.1109/MSP.2008.926663.
9. Xiao, D., Kang, X., Li, Y., Wu, W., Fang, D. (2019). Insight into the negative Poisson's ratio effect of metallic auxetic reentrant honeycomb under dynamic compression. *Materials Science and Engineering: A*, 763, 138151. DOI 10.1016/j.msea.2019.138151.
10. Hu, L. L., Zhou, M. Z., Deng, H. (2018). Dynamic crushing response of auxetic honeycombs under large deformation: Theoretical analysis and numerical simulation. *Thin Walled Structures*, 131(10), 373–384. DOI 10.1016/j.tws.2018.04.020.
11. Hou, X., Deng, Z., Zhang, K. (2016). Dynamic crushing strength analysis of auxetic honeycombs. *Acta Mechanica Sinica*, 29(5), 490–501. DOI 10.1016/S0894-9166(16)30267-1.
12. Tan, H. L., He, Z. C., Li, K. X., Li, E., Cheng, A. G. et al. (2019). In-plane crashworthiness of re-entrant hierarchical honeycombs with negative Poisson's ratio. *Composite Structures*, 229(12), 111415 1–111415 15. DOI 10.1016/j.compstruct.2019.111415.
13. Dong, Z., Li, Y., Zhao, T., Wu, W., Liang, J. (2019). Experimental and numerical studies on the compressive mechanical properties of the metallic auxetic reentrant honeycomb. *Materials & Design*, 182, 108036. DOI 10.1016/j.matdes.2019.108036.
14. Sun, Y., Pugno, N. M. (2013). In plane stiffness of multifunctional hierarchical honeycombs with negative Poisson's ratio sub-structures. *Composite Structures*, 106(12), 681–689. DOI 10.1016/j.compstruct.2013.05.008.
15. Lu, Z. X., Li, X., Yang, Z. Y., Xie, F. (2016). Novel structure with negative Poisson's ratio and enhanced young's modulus. *Composite Structures*, 138(3), 243–252. DOI 10.1016/j.compstruct.2015.11.036.
16. Fu, M. H., Zheng, B. B., Li, W. H. (2017). A novel chiral three-dimensional material with negative Poisson's ratio and the equivalent elastic parameters. *Composite Structures*, 176(9), 442–448. DOI 10.1016/j.compstruct.2017.05.027.
17. Li, D., Yin, J., Dong, L., Lakes, R. S. (2017). Numerical analysis on mechanical behaviors of hierarchical cellular structures with negative Poisson's ratio. *Smart Material Structures*, 26(2), 025014. DOI 10.1088/1361-665X/26/2/025014.
18. Hou, J., Li, D., Dong, L. (2018). Mechanical behaviors of hierarchical cellular structures with negative Poisson's ratio. *Journal of Materials Science*, 53(14), 10209–10216. DOI 10.1007/s10853-018-2298-0.
19. Zhang, X., An, C., Shen, Z., Wu, H., Yang, W. et al. (2020). Dynamic crushing responses of bio-inspired re-entrant auxetic honeycombs under in-plane impact loading. *Materials Today Communications*, 23, 100918. DOI 10.1016/j.mtcomm.2020.100918.

20. Xu, C., Pang, T., Kang, H. (2019). Crashworthiness research and design of thin-walled s-shaped beams with variable cross-section. *Machinery Design and Manufacture*, (2), 100–103,106.
21. Zhang, Y., Xu, X., Li, Q., Lu, M., Liao, S. (2017). Study on Crashworthiness of Novel multi cell thin-walled structures with variable cross-section. *China Journal of Highway and Transport*, 30(7), 151–158.
22. Xiaofei, C., Shengyu, D., Jun, L., Weibin, W., Daining, F. (2018). Mechanical properties of an improved 3d-printed rhombic dodecahedron stainless steel lattice structure of variable cross section. *International Journal of Mechanical Sciences*, 145, 53–63. DOI 10.1016/j.ijmecsci.2018.07.006.
23. Liu, Y., Wu, H. X., Wang, B. (2012). Gradient design of metal hollow sphere (mhs) foams with density gradients. *Composites Part B*, 43(3), 1346–1352. DOI 10.1016/j.compositesb.2011.11.057.
24. Zhang, X. C., An, L. Q., Ding, H. M., Zhu, X. Y., El-Rich, M. (2014). The influence of cell micro-structure on the in-plane dynamic crushing of honeycombs with negative Poisson's ratio. *Journal of Sandwich Structures and Materials*, 17(1), 26–55. DOI 10.1177/1099636214554180.